Published in final edited form as:
J Immunol. 2009 August 15; 183(4): 2554–2564. doi:10.4049/jimmunol.0901276.

Structural basis of the CD8αβ/MHCI interaction: focused recognition orients CD8β to a T cell proximal position[1]

Rui Wang[*], **Kannan Natarajan**[2,*], and **David H. Margulies**[2,*]

[*]Molecular Biology Section, Laboratory of Immunology, National Institute of Allergy and Infectious Diseases, National Institutes of Health, Bethesda, MD 20892-1892

Abstract

In the immune system, B cells, dendritic cells, NK cells, and T lymphocytes all respond to signals received via ligand binding to receptors and coreceptors. While the specificity of T cell recognition is determined by interaction of T cell receptors with MHC/peptide complexes, the development of T cells in the thymus and their sensitivity to antigen are also dependent on coreceptor molecules CD8 (for MHCI) and CD4 (for MHCII). The CD8αβ heterodimer is a potent coreceptor for T cell activation, but efforts to understand its function fully have been hampered by ignorance of structural details of its interactions with MHCI. Here we describe the structure of CD8αβ in complex with the murine MHCI molecule H-2D^d at 2.6 Å resolution. The focus of the CD8αβ interaction is the acidic loop (residues 222-228) of the α3 domain of H-2D^d. The β subunit occupies a T cell membrane-proximal position, defining the relative positions of the CD8α and CD8β subunits. Unlike the CD8αα homodimer, CD8αβ does not contact MHCIα2 or β2-microglobulin domains. Movements of the CD8α complementarity determining region-(CDR) 2 and CD8β CDR1 and CDR2 loops as well as flexibility of the H-2D^d CD loop facilitate the monovalent interaction. The structure resolves inconclusive data on the topology of the CD8αβ/MHCI interaction, indicates that CD8β is crucial in orienting the CD8αβ heterodimer, provides a framework for understanding the mechanistic role of CD8αβ in lymphoid cell signaling, and offers a tangible context for design of structurally altered coreceptors for tumor and viral immunotherapy.

Keywords

cell surface molecules; T cells; MHC; T cell receptors

Introduction

The recognition of cell surface MHC-peptide complexes by T cells lies at the heart of the adaptive immune response. Specific identification of MHC-peptide complexes is mediated by the immunoglobulin-like, clonotypic α and β chains of the TCR and components of the multi-subunit CD3 complex that transduce signals to the T cell. However, TCR/MHC-peptide interactions alone do not efficiently trigger T cells, necessitating the engagement of the T cell coreceptors CD8 or CD4 by MHCI or MHCII respectively on the presenting cell, for potent T cell activation (1-3). Engagement of CD8 recruits the Src family kinase Lck to the TCR

[1]This research was supported by the Intramural Research Program of the NIAID, National Institutes of Health.

2Address correspondence and reprint requests to Dr. Kannan Natarajan, or Dr. David H. Margulies, Molecular Biology Section, Laboratory of Immunology, National Institute of Allergy and Infectious Diseases, National Institutes of Health, Bldg. 10, Room 11N311; 10 Center Drive, Bethesda, MD 20892-1892. knatarajan@niaid.nih.gov and dhm@nih.gov.

Disclosures
The authors have no financial conflict of interest.

signalling complex, augmenting a stimulatory cascade (4) that involves conformational changes in the cytoplasmic tyrosine-based motifs of chains in the CD3 complex(5,6). CD8/MHCI interactions play two overlapping roles: one related to the direct participation of CD8 as a component of the TCR/MHC signaling complex (coreceptor function) (7-11); and a second in which binding to neighboring MHC molecules contributes to stabilization of the T cell/antigen presenting cell (APC) interface (accessory function)(12-15). As a cell surface disulfide-linked dimeric glycoprotein, CD8 occurs in CD8αα and CD8αβ isoforms, which have distinct cellular distribution and function. CD8αα is broadly distributed and is found on intestinal intraepithelial lymphocytes, γδ T cells, subsets of dendritic cells, and NK cell subpopulations. The coreceptor function of CD8αα has been re-examined (16), and it has been proposed recently that CD8αα may negatively regulate cell activation in some lymphoid cell subsets (17). In contrast, CD8αβ is expressed by αβ TCR thymocytes and mature peripheral αβ T cells where it is indispensable for thymic selection of CD8 T cells (18-20) as well as for activation of peripheral CD8 T cells (21,22). By linking thymic MHC recognition and TCR signaling, CD8αβ guides the developing TCR repertoire towards appropriate self-MHC recognition (23).

Despite the critical importance of CD8αβ for normal T cell development and function, the molecular basis for its biological differences from CD8αα is still clouded in controversy. A number of laboratories have evaluated biophysical parameters of binding of CD8αα and CD8αβ for MHCI, resulting in the general acceptance that, despite clear differences in function, both isoforms bind MHCI with essentially the same affinity. This binding is consistently observed to be independent of the nature of the particular MHC-bound peptide, although there are clear differences among MHCI alleles (7,10,24-26). Recently, measurement of the two-dimensional kinetics of the cell surface constrained CD8/MHCI interaction led to generally the same conclusions that CD8αα and CD8αβ interact with MHCI in an allele dependent but TCR and peptide independent manner (27). Experiments using a set of chimeric murine β chains expressed in CD8β–deficient mice suggest that the functional avidity advantage of CD8αβ derives from contributions of both its ectodomain and its cytoplasmic domain (2,28, 29).

CD8 α and β chains consist of an Ig-like domain that is linked via a stalk to a transmembrane domain and a cytoplasmic tail. The tail serves CD8α as an Lck docking site. The superior coreceptor activity of CD8αβ has been attributed to the stalk region of the β chain and its glycosylation (30-33) and to a palmitoylation site in the β cytoplasmic tail (11), which targets CD8αβ and the associated TCR to lipid rafts. Recent studies indicate that a conserved peptide motif of the TCR α chain connecting peptide plays a crucial role in CD8β participation in signal transduction (34).

Extensive analyses of polymorphic variants and single site mutants of MHCI (35-40) and CD8 (41), initially guided by the MHCI structures, and subsequently by structures of CD8αα/MHCI complexes, have identified key residues mediating this interaction. However, the lack of a definitive structure of an MHCI/CD8αβ complex has hampered the interpretation of such data. Consideration of the surface electrostatic charge of the original HLA-A2/CD8αα structure led to speculation that CD8αβ would bind in the same general position and orientation, with the CD8β subunit replacing the CD8α2, in a T cell distal position (42). Early mutational studies suggested a similar orientation (43). However, consideration of the differences in the length of the stalk region of CD8α as compared to CD8β prompted others to favor the opposite orientation (26), with the CD8β chain in the T cell proximal CD8α1 location. Further mutational analyses of the HLA-A2/CD8 and H-2K^b/CD8 interactions provoked the unusual hypothesis that CD8αβ might bind MHCI in two distinct orientations (44,45). To clarify the role of CDαβ in providing coreceptor signals, to illuminate structural aspects of the contribution of CDαβ to T cell development and activation, and to resolve ambiguities inherent in the

interpretation of mutagenesis data, we have determined the structure of murine CD8αβ in complex with H-2D^d at 2.6 Å resolution. For comparison with an unliganded MHCI molecule, we also report a new high resolution (1.7 Å) structure of an H-2D^d/β2m/peptide complex. These structural data are further employed to interpret extensive mutational data in the literature.

Materials and Methods

Protein Expression and Purification

Bacterial expression and purification of the H-2D^d/mβ2m/P18I10 complex have been described earlier (46). Expression and purification of H-2K^b/mβ2m/ISFK8 followed the same protocol. (The ISFK8 peptide, ISFKFDHL, has been described previously (47)). For mouse CD8αβ, *E. coli* codon-optimized DNA sequences encoding their extracellular domains were chemically synthesized (Genscript Corporation, Piscataway, NJ), separately subcloned into the pET21b bacterial expression vector (Novagen, EMD Chemicals, San Diego, CA), and transformed into *E. coli* Rosetta 2 (Novagen). The codon-optimized DNA sequences are included as Supplementary Figure 1, and have been deposited in GenBank (accession numbers GQ247790, GQ247791). The encoded protein extends from Gly -5 to Gly161 for CD8α and from Ser -3 to Gly147 for CD8β. This numbering scheme preserves that previously used for mouse CD8αα and CD8αβ structures (48,49), which begin with Lys1 and Leu1 for CD8α and β respectively. CD8α and β were separately expressed with the Overnight Express Autoinduction System (Novagen). Inclusion bodies containing CD8α and CD8β protein obtained from 500 mL expression cultures were each denatured in 10 mL of 6M guanidine-HCl in TRIS-EDTA buffer pH8 containing 0.1mM dithiothreitol. Insoluble material was spun out, the supernatants mixed together, and added dropwise over 15 min to 1 L of chilled refolding buffer (0.4M arginine hydrochloride, 100mM TRIS pH8, 2mM EDTA, 3mM reduced glutathione, and 0.3mM oxidized glutathione). After incubation for four days at 4°C, the solution was dialyzed against 25mM MES pH5.5, concentrated and bound to a Hi-Trap SP cartridge (Pharmacia), and then eluted in MES buffer containing 1M NaCl. After overnight dialysis against 25mM HEPES pH7, 150mM NaCl, the protein was subjected to size exclusion chromatography on a Superdex 75 column in the same buffer. The major peak with the predicted retention time of the dimer was recovered and dialyzed against 25mM HEPES pH7, 50mM NaCl. The protein was then subjected to ion-exchange chromatography on a mono S column (Pharmacia) developed with a 0.05M-0.5M NaCl gradient in 25mM HEPES pH7. Two major peaks were resolved with the disulfide-linked CD8αα homodimer eluting earlier in the NaCl gradient than the disulfide-linked CD8αβ heterodimer. SDS-PAGE under reducing and nonreducing conditions revealed the disulfide linkage. Edman degradation sequencing of the amino terminal 15 residues confirmed the localization of the CD8αα and CD8αβ dimers to the earlier and later peaks, respectively, on mono S chromatography. The αα homodimer peak constituted 35 to 40% of the total protein in the two peaks. The CD8αβ peak was collected, the salt concentration adjusted to 50mM by dilution, and protein was concentrated to 10mg/ml for crystallization trials. In experiments requiring CD8αα the α chain alone was expressed, refolded, and purified as described above.

Analysis of binding by surface plasmon resonance (SPR)

Surface plasmon resonance binding experiments were performed on a BIAcore™ 2000, CM-5 chip surfaces of which were covalently coupled with either CD8αα or CD8αβ. Data were analyzed with BIAeval 3.2. Coupling conditions and data analysis were as described previously for TCR (50).

Crystallization and Data Collection

The CD8αβ/H-2D^d complex was crystallized using the hanging-drop vapor diffusion method at room temperature. The H-2D^d/mβ2m/P18I10 complex and the CD8αβ heterodimer were

mixed in a 1 to 2 molar ratio to a final protein concentration of 5 mg/ml, and crystals formed within one month in 12% PEG 3000, 50mM HEPES, pH7.5. A single crystal of 0.1 × 0.1 × 0.1 mm was frozen in liquid nitrogen after dipping in Paratone-N. X- ray diffraction data were collected under a nitrogen stream at 100 K at beamline 22ID-D at the Advanced Proton Source at Argonne National Laboratory, at a wavelength of 1.0 Å, using a MAR300 detector. The data were indexed, integrated, scaled and merged with HKL2000(51). The statistics of the crystallographic data collection are summarized in Table I.

For unliganded H-2D^d/mβ2m/P18I10, crystals were grown at room temperature in hanging drops over 16% PEG-3350 containing 0.2M magnesium formate, and cryopreserved in liquid nitrogen. Diffraction data to 1.7 Å were collected on a single crystal at beamline X29 at the National Synchrotron Light Source, Brookhaven, using a ADSC Quantum-315r CCD detector. Data were processed with HKL2000 and the structure was solved by molecular replacement. Data collection and refinement statistics are reported in Table I.

Structure Determination

The structure of the CD8αβ/H-2D^d complex was determined by molecular replacement using the programs MOLREP (52) and Phaser (53) of the CCP4 suite (54) with the H-2D^d/P18I10 portion of the H-2D^d/P18I10/Ly49A complex (55) (PDB (56) code 1QO3) and mouse CD8αβ (49) (PDB code 2ATP) as search models, respectively. The crystal belonged to the space group $P2_12_12_1$ with one complex (H-2D^d heavy chain, β2m, P18I10, CD8α, and CD8β) in the asymmetric unit. The structure of unliganded H-2D^d/mβ2m/P18I10 was solved by molecular replacement with AMORE (54) using our previously determined H-2D^d/P18I10 structure (1DDH)(46) as a search model.

Model Building, Refinement, and Structure Analysis

For the CD8αβ/H-2D^d dataset, after an initial round of rigid body refinement, the model was fitted manually with Coot (57). The structure was refined with simulated annealing, energy minimization, B factor refinement and water addition using CNS (58). The final model with an R_{work} of 24.8 and R_{free} of 29.2 was obtained. The first three N-terminal residues (Lys-Pro-Gln) of CD8α were not visualized, and the first residue of the mature CD8β (Leu1) was in good density. Part of the C-terminal stalk region (Asp-Val-Leu-Pro) of CD8β was seen and built into the model. Uninterrupted electron density was observed for H-2D^d heavy chain residues 2 to 275, β2m light chain residues -1 to 99, and the decamer peptide, as well as for CD8α residues 4 to 122 and CD8β residues 1 to 120. However, although backbone density was observed for CD8α Leu69 to Phe75 and Leu89 to Lys91, side chain density was indistinct. No electron density was visible for the bulk of the stalk regions of either CD8 subunit.

For unliganded H-2D^d/mβ2m/P18I10 the refinement steps and water addition were carried out in PHENIX (59) followed by inspection of the maps in Coot. Anisotropic refinement of B factors was included in view of the relatively high resolution of this dataset.

Analysis of the resulting structures was accomplished with programs in CCP4 (54) and PDBsum(60). All molecular graphics figures were generated with PyMOL (http://www.pymol.org). Coordinates and structure factors have been deposited with the protein data bank (PDB) with accession codes 3DMM (CD8αβ/H-2D^d) and 3ECB (H-2D^d/β2m/P18I10), and can be accessed at http://www.rcsb.org (56).

Results

Engineering soluble CD8αβ for binding and crystallization

Bacterial expression constructs encoding the extracellular portion of CD8α and β, including the first interchain disulfide, were expressed in *E. coli* and purified (see Materials and Methods and Supplemental Figure 1). Surface plasmon resonance (SPR) binding studies, using either the CD8αβ heterodimer or a similarly engineered CD8αα homodimer and recombinant H-2D^d and H-2K^b, revealed affinity constants (K_D) for these carbohydrate-free, disulfide-linked CD8 proteins of 6.7 to 38.4 μM (Figure 1). The measured solution affinities are similar to those reported by some (7), but greater than those measured by others for mouse (61) and human (10, 62) molecules, and may reflect differences among MHC molecules (27). We observe little difference in the apparent affinity of CD8αβ as compared with CD8αα for MHCI, consistent with previous findings (7, 27, 63). In addition, comparisons of binding of H-2D^d complexes prepared with different peptides revealed no significant difference in binding to CD8αβ, consistent with the accepted view that the influence of peptide is minimal (7, 27, 64) (data not shown).

Overall structure of the CD8αβ/H-2D^d complex

Crystallization conditions for the complex of H-2D^d with CD8αβ were determined, and synchrotron diffraction data to 2.6 Å were collected (see Materials and Methods and Table I). The structure, solved by molecular replacement, revealed continuous electron density for all five chains of the complex (CD8α, CD8β, H-2D^d, β2m, and the P18I10 peptide), but no density was visible for the bulk of the stalk regions of either CD8 chain. CD8α chain density extended from residue 4 to 121, and CD8β from 1 to 123. The overall complex, roughly 70 Å by 70 Å by 60 Å, reveals the canonical MHCI/β2m/peptide complex, bound to the two Ig-like domains of CD8α and CD8β (Figure 2A). The CD8αβ heterodimer focuses on the α3 domain of the H-2D^d heavy chain, consistent with early studies that mapped the binding site using mouse and human MHC variants (35,36). CD8β is located in a position equivalent to that of the CD8α1 subunit of the three CD8αα/MHC complex structures (CD8αα/H-2K^b (48), CD8αα/TL (65), and CD8αα/HLA-A2 (42) (Figure 3). This region lies adjacent to, but not touching, the MHCI α2 domain platform, in an “upper”, T cell proximal, position. CD8α occupies the same relative position as the CD8α2 subunit of the CD8αα complexes, and is positioned closer to the carboxyl-terminus of the H-2D^d α3 domain, in a T cell distal location.

Although the recombinant CD8αβ protein contained residues of the stalk that join the Ig-like domains to the transmembrane region, the electron density map revealed very little of this region, presumably due to flexibility of this part of the molecule. However, the first several residues of the CD8β chain stalk, extending to CD8β Pro123 were visualized. These residues (from Pro123 on) seem to point towards the T cell. The disposition of the H-2D^d α3 domain relative to the peptide-binding α1α2 domain, and the relationship of the β2m subunit to the MHCI heavy chain are conserved in this complex structure.

The CD8αβ/H-2D^d interface

The CD8αβ heterodimer only contacts H-2D^d residues located on the α3 domain (see Figure 2 and Table II). This contrasts with CD8αα which also makes contact with residues of the MHCI α2 and β2m domains. The exclusive focus of CD8αβ on the α3 domain of H-2D^d decreases the buried surface between CD8αβ and H-2D^d to 963 Å^2, which differs from the buried surfaces of H-2K^b, TL, and HLA-A2 in complex with CD8αα of 1756, 1855, and 1302 Å^2 respectively (Table III). The shape complementarity statistic (Sc)(66), an indicator of three-dimensional fit of a ligand for its receptor, calculated for the interface between the CD8 heterodimer and the MHC heavy chain is 0.59 for the CD8αβ/H-2D^d complex which is similar to that calculated for CD8αα/H-2K^b (0.61) and CD8αα/TL (0.65), but less than that calculated

for CD8αα/HLA-A2 (0.72). The CD8β subunit of CD8αβ contributes almost equally (49%) to the buried surface of the interface. This contrasts to the three CD8αα/MHC complexes in which the CD8α1, "upper", subunit contributes the bulk of the buried surface area (69%, 71%, and 74% of the interface for H-2K^b, TL, and HLA-A2 respectively). In the three CD8αα/MHC structures, residues of the three CDR loops of CD8α1 and of the N-terminus bind through hydrogen bonds and atomic contacts to both the MHC α3 domain and also to β2m. The footprint of CD8αβ on H-2D^d is compared graphically with that of CD8αα on H-2K^b in Figure 3E and F, emphasizing the more extensive interactions of CDα1 with residues of β2m as well as with H-2K^b residues of the α2 and α3 domains. In addition, the CD8α2 subunit (of CD8αα) interacts over a larger surface area and with more residues of the H-2K^b α3 domain as compared with the CD8α subunit's interactions with H-2D^d. In contrast, in the CD8αβ/H-2D^d complex only five residues of CD8β: one in the CDR1 loop (Lys27), three in the CDR3 loop (Gly100, Ser101, and Pro102), and one in β-strand F (Val99) contact H-2D^d (see Table II and Figure 2E). Ser101 and Pro102 participate via hydrogen bonds whose focus is on Thr225 and the highly conserved Gln226 of the H-2D^d α3 domain (Figure 2C and Figure 4A). Although CDR1 of CD8β makes contact through residue Lys27 to H-2D^d α3 domain residues Asp212 and Thr214, its CDR2 makes none at all (Table II). Of the residues of the H-2D^d α3 domain that interact with CD8αβ (Table II and Figure 4), Gln226 is the only one that interacts with both subunits (Figure 2C and Figure 3E and F). The footprint of the CD8α subunit on the α3 domain (Figure 2C and E, Figure 3E and F) is only slightly altered compared to that of its counterpart, the CD8α2 (lower) subunit in the CD8αα/H-2K^b complex (Figure 2A and B).

Superposition of the bound and free forms of CD8αβ reveals differences in the CDR1 and CDR2 loops of CD8β as well as the CDR2 loop of CD8α (Figure 5). These loops adjust and are stabilized by interaction with the H-2D^d α3 domain. The largest adjustments are in CD8β CDR1 where the Cα atom of residue Lys27 is displaced by 2.9 Å and its Nζ atom by 8.8 Å in the liganded structure (Figure 5D and E). Also, His60 of CD8α CDR2 approaches H-2D^d residue Glu227 in the bound structure. Notably, all CDR adjustments move the loops farther away from each other in the bound as compared to the unbound state. (The minor change in disposition of the DE loop of CD8α (Figure 5A) is not directly related to interaction with H-2D^d). These apparent adjustments of the loops of CD8β and of CD8α suggest that mobility of these loops permits a degree of "adaptive fit" to facilitate the interaction of the CD8 heterodimer with the MHC α3 domain. Changes in H-2D^d in the free and bound states are noted below.

Although the structure of unliganded H-2D^d has been determined previously (46,67), for more precise comparison with the CD8αβ/H-2D^d complex we have determined the structure of the H-2D^d/mβ2m/P18I10 complex to 1.7 Å resolution (see Table I). Inspection of the 222–228 loop of the α3 domain of H-2D^d of the CD8-bound and free forms reveals mobility, particularly of the side chains of Gln226 and Glu227 (Figure 4C), which adapt to the pocket formed by the CD8αβ CDRs. Comparison of the hinge angle between the α1α2 domain platform and the α3 domain of H-2D^d in the CD8αβ bound state with the high resolution H-2D^d structure reveals slight movement of the α3 domain away from the platform domain by 6°, resulting in a larger angle for the bound versus free form of H-2D^d (76° and 70° respectively). This angle in the CD8αβ/H-2D^d complex is similar to that of H-2D^d bound to the Ly49A NK receptor (hinge angle of 77°), which binds in a similar region (55). As expected, interaction of CD8αβ with H-2D^d has essentially no effect on the conformation of the α1α2 domain and the bound peptide. (Superposition of this region has an rmsd of 0.44 Å for 189 superposed Cα atoms).

Discussion

Rationalization of mutagenesis data on the CD8αβ/MHC-I interaction

The crystal structure of the CD8αβ/H-2D^d complex now enables rationalization of extensive mutational analyses of the relative contributions of residues of CD8α and CD8β to binding and coreceptor functions (see Table IV). The structure emphasizes the critical role of the CD8β and CD8α CDR3 loops, both clamping down on the finger-like protrusion of H-2D^d residue Gln226 (Figure 2C, Figure 4, and Table II). Different laboratories have employed distinct assays of CD8/MHCI interactions: MHCI/peptide tetramer staining (65,68), antigen-specific T cell hybridoma activation (32,44,49), and alloreactive and antigen specific T cell activation (13,36,37,39,69). Many of the effects of mutations observed in these assays can be explained either by previously reported CD8αα/MHCI structures or by the CD8αβ/MHCI structure reported here (Table IV). Mutations of CD8 and MHCI and polymorphisms of MHCI have been studied extensively. A number of CD8α mutants have been examined--those that decrease binding of transfectants by TL/β2m tetramers can be readily explained as mutants that affect contact residues to either CD8α1 or CD8α2 subunits (see Table IV). Although several mutations of CD8α that decrease binding by H-2K^b tetramers (Asn107Ala, Lys62Glu, Ser31Leu or Ala, Arg8Asp or Ala) can be rationalized because these are contact residues to either MHC or β2m, several others (Thr81Ala, Leu29Ala, and Lys12Glu) cannot be easily explained, although Thr81 resides at the edge of the H-2K^b interface with CD8α1. More interesting and also not easy to explain is the apparent augmentation of binding observed with the CD8α Lys73Ala mutant. This side chain is exposed to solvent on the backside C′ C″ loop, and thus cannot directly influence MHC interaction. Functional effects of Arg8Ala and Glu27Ala substitutions can be explained as these CD8α residues (in the CD8α1 subunit) contact β2m. (The residues of β2m involved are Lys58 and Asp59. Lys58 is conserved in the human β2m used for some tetramers, and Asp59 is substituted by Asn (in human β2m) which preserves size and hydrogen bonding ability).

A number of CD8β mutants, designed primarily because of their location in CDR loops of CD8β, have been examined both in tetramer binding (45) and in T cell hybridoma stimulation assays (44,49). Mutants of CDR3β (Ser101Ala, Val99Arg, Pro102Ala) that diminish binding or functional activity are readily explained because the parental side chain interacts with MHC residues at or near the conserved MHCI Gln226 focus. The Oγ atom of Ser101 forms a hydrogen bond with the carbonyl oxygen of Thr225 of the H-2D^d α3 domain (Table II), an interaction that is eliminated by the Ser101Ala substitution. The CD8β Pro102Ala mutation, of a residue that contacts Gln226, also abrogated both CD8 coreceptor and binding activity (45,49,70). Mutation of the adjacent Lys103 to Ala reduced but did not abolish the activity of CD8αβ (45). Mutants of CDR3β Lys103, to either Asp or Ala, can be explained despite the lack of direct contact of the Lys sidechain with H-2D^d. The Lys103 sidechain is positioned to make a long range ion pair with CD8α Asp66 (Lys103/Nζ is 4.0 Å from Asp66/Oδ1). Indeed, in the structure of the unliganded mouse CD8αβ (49) this bridge is shorter, and involves both Asp66 carboxylate oxygens. Thus, we may speculate that CD8β Lys103 plays an important role in stabilization of the CD8αβ heterodimer. The CD8β Val99Arg mutation reduced staining in a tetramer-binding assay, a result that may be due to conformational effects on the CD8β CDR3 loop resulting from introduction of the long Arg side chain (45). CD8β CDR2 mutants have varied effects (44,45,49), perhaps because the CDR2 contacts to H-2D^d are more peripheral to the Gln226 focus. CD8β Lys55Asp and mutation of Gly56, Lys55, Ser54 and Ser53 to Ala all result in decreased tetramer binding or reduced T cell hybridoma stimulation (see Table IV). At first glance all of these are difficult to explain based on the structure of the complex, but on closer scrutiny we note that Lys55, which does not contact H-2D^d, clearly interacts with CD8α Ser108. Similar to the role of CD8β Lys103, Lys55 is involved in a heterodimer interdomain interaction, suggesting again that dimer stability is important in CD8αβ function.

Point mutations of CD8β CDR1 have little or no effect, although the single CD8β CDR1 contact residue observed in the structure, Lys27, was not tested directly (45,49). However, in the CD8αβ heterodimer interface this residue forms hydrogen bonds with Ser108 of CD8α. Thus, its mutation may destabilize the CD8αβ heterodimer. Some of the interactions of CD8α Ser108 with the CD8 β chain are illustrated in Supplemental Figure 2. Other CD8β mutants of residues not involved in MHC binding that have significant functional effects can also be explained by their role in disruption of heterodimer stability (Table IV).

Several mutants of CD8 are known to improve CD8αβ dependent T cell activation or binding to tetramers. In particular, CD8α Lys73Ala and CD8β Leu58Arg and Ser53Leu augmented binding of H-2K^b tetramers (45,68). Perhaps elimination of the Lys73 to Asn90 hydrogen bond provided greater flexibility, allowing better accommodation of interaction. Leu58 is a contact residue to CD8α Ser108, and one might consider that the substitution by Arg would stabilize the heterodimer. CD8β Ser53Leu substitution may contribute to stabilization of the CD8β CDR2 loop. Recent studies of engineered TCR indicate that improvement of TCR αβ heterodimer stability by introduction of subunit bridging disulfide bonds contributes to the improvement of both expression and biological activity (71,72). Our interpretation of changes of activity of CD8α and β mutants in the context of the structure of the CD8αβ/MHCI complex suggests that other mutations that might stabilize the CD8αβ heterodimer (such as introduction of interdomain salt bridges or disulfide bonds) might also lead to improved MHC binding and accessory function.

Examination of structure based amino acid sequence alignments of CD8α, CD8β, and the MHCI α3 domain offers additional insight into the conservation of the structure of the complex in other species (Figure 6). N-linked carbohydrate addition sites of both CD8α and β do not impinge on the interface with MHCI. Few contact residues of CD8β are particularly polymorphic, with the exception of Lys27, which is preserved in rodents. A major contact loop of CD8β, consisting of residues 99 to 102 (CDR3, FG loop), is highly conserved. Considerable effort has been expended to understand the molecular basis for the apparent higher affinity of the MHCI-like TL molecule for CD8αα as compared with CD8αβ (81). Examination of the CD8αβ/H-2D^d structure in comparison with CD8αα/TL and inspection of MHCI α3 domain sequences (Figure 6) suggest that the substitution of His in TL for Asp212 in H-2D^d, a residue that contacts Lys27 of CD8β, may play a significant role. Additional experiments will be needed to address this issue.

Clear definition of “upper” position of the CD8β domain

The structure reported here defines a single orientation of CD8αβ binding to MHCI, in which the β subunit occupies the “upper,” T cell proximal, CD8α1-equivalent position. Consideration of surface electrostatic interactions of CD8αα with HLA-A2 led to the suggestion that the CD8β subunit occupies the “lower”, T cell distal, CD8α2-equivalent, position (42) and mutagenesis data suggested a dual orientation model, in which the CD8β subunit can dynamically alternate between the “upper” and “lower” positions (44,45). Although it is difficult to formally eliminate the dual conformation model, we emphasize that crystallographic capture of a single orientation CD8β in the T cell proximal position, that is consistent with most of the existing mutagenesis data argues strongly against such a model. Moreover, to our knowledge there is no precedent in the extensive literature on protein:protein interactions for a heterodimeric receptor that binds in dual, inverse orientations to the same ligand. Because of the sequence similarities of murine and human MHCI molecules as well as the similarities among species of CD8α and of CD8β (Figure 6), we expect that the domain relationships of the murine structure we report here are preserved in the CD8αβ/MHCI complexes of other species. Additional perspective gained from consideration of relative sizes of the subunits of a complete TCR/MHCI/CD8 complex may be gathered from the

superposition of the structure of a TCR/H-2D^d complex (KN and DHM, unpublished) onto the CD8αβ/H-2D^d structure reported here (Figure 7). Although the role of CD8αβ as a T cell coreceptor dictates its "trans" interaction with the peptide-binding MHCI molecule on the APC, we note that the structure of the CD8αβ/MHCI complex does not eliminate the possibility of a "cis" interaction between CD8αβ and MHCI expressed on the T cell (73-76). Our structural analysis is consistent with the view that the shorter stalk of CD8β plays a crucial role in the orientation of the cytoplasmic domains of the CD8αβ heterodimer for their role in signal transduction (33). The structure of this murine CD8αβ/MHCI complex may serve as a guide to a mechanistic understanding of human CD8 mutants that result in immunodeficiency (77, 78) and provide a context for further examination of the role of the distinct domains of the CD8 molecule in binding and function.

Supplementary Material

Refer to Web version on PubMed Central for supplementary material.

Acknowledgments

We thank Zhongmin Jin of SER-CAT of the Advanced Photon Source at Argonne National Laboratory and Howard Robinson at beamline X29 at the National Synchrotron Light Source, Brookhaven, for data collection, and John E. Coligan and Sam Xiao for their comments on the manuscript.

References

1. Laugel B, van den Berg HA, Gostick E, Cole DK, Wooldridge L, Boulter J, Milicic A, Price DA, Sewell AK. Different T cell receptor affinity thresholds and CD8 coreceptor dependence govern cytotoxic T lymphocyte activation and tetramer binding properties. J Biol Chem 2007;282:23799–23810. [PubMed: 17540778]
2. Singer A, Bosselut R. CD4/CD8 coreceptors in thymocyte development, selection, and lineage commitment: analysis of the CD4/CD8 lineage decision. Adv Immunol 2004;83:91–131. [PubMed: 15135629]
3. Zamoyska R. CD4 and CD8: modulators of T-cell receptor recognition of antigen and of immune responses? Curr Opin Immunol 1998;10:82–87. [PubMed: 9523116]
4. Chan IT, Limmer A, Louie MC, Bullock ED, Fung-Leung WP, Mak TW, Loh DY. Thymic selection of cytotoxic T cells independent of CD8 alpha-Lck association. Science 1993;261:1581–1584. [PubMed: 8372352]
5. Xu C, Gagnon E, Call ME, Schnell JR, Schwieters CD, Carman CV, Chou JJ, Wucherpfennig KW. Regulation of T cell receptor activation by dynamic membrane binding of the CD3epsilon cytoplasmic tyrosine-based motif. Cell 2008;135:702–713. [PubMed: 19013279]
6. Aivazian D, Stern LJ. Phosphorylation of T cell receptor zeta is regulated by a lipid dependent folding transition. Nat Struct Biol 2000;7:1023–1026. [PubMed: 11062556]
7. Garcia KC, Scott CA, Brunmark A, Carbone FR, Peterson PA, Wilson IA, Teyton L. CD8 enhances formation of stable T-cell receptor/MHC class I molecule complexes. Nature 1996;384:577–581. [PubMed: 8955273]
8. Cole DK, Gao GF. CD8: adhesion molecule, co-receptor and immuno-modulator. Cell Mol Immunol 2004;1:81–88. [PubMed: 16212893]
9. Gakamsky DM, Luescher IF, Pramanik A, Kopito RB, Lemonnier F, Vogel H, Rigler R, Pecht I. CD8 kinetically promotes ligand binding to the T-cell antigen receptor. Biophys J 2005;89:2121–2133. [PubMed: 15980174]
10. Wyer JR, Willcox BE, Gao GF, Gerth UC, Davis SJ, Bell JI, van der Merwe PA, Jakobsen BK. T cell receptor and coreceptor CD8 alphaalpha bind peptide-MHC independently and with distinct kinetics. Immunity 1999;10:219–225. [PubMed: 10072074]
11. Arcaro A, Gregoire C, Bakker TR, Baldi L, Jordan M, Goffin L, Boucheron N, Wurm F, van der Merwe PA, Malissen B, Luescher IF. CD8beta endows CD8 with efficient coreceptor function by

coupling T cell receptor/CD3 to raft-associated CD8/p56(lck) complexes. J Exp Med 2001;194:1485–1495. [PubMed: 11714755]

12. Knall C, Ingold A, Potter TA. Analysis of coreceptor versus accessory molecule function of CD8 as a correlate of exogenous peptide concentration. Mol Immunol 1994;31:875–883. [PubMed: 8065371]
13. Shen L, Potter TA, Kane KP. Glu227-->Lys substitution in the acidic loop of major histocompatibility complex class I alpha 3 domain distinguishes low avidity CD8 coreceptor and avidity-enhanced CD8 accessory functions. J Exp Med 1996;184:1671–1683. [PubMed: 8920857]
14. Belyakov IM, Kozlowski S, Mage M, Ahlers JD, Boyd LF, Margulies DH, Berzofsky JA. Role of alpha3 domain of class I MHC molecules in the activation of high- and low-avidity CD8+ CTLs. Int Immunol 2007;19:1413–1420. [PubMed: 17981793]
15. Yachi PP, Ampudia J, Gascoigne NR, Zal T. Nonstimulatory peptides contribute to antigen-induced CD8-T cell receptor interaction at the immunological synapse. Nat Immunol 2005;6:785–792. [PubMed: 15980863]
16. McNicol AM, Bendle G, Holler A, Matjeka T, Dalton E, Rettig L, Zamoyska R, Uckert W, Xue SA, Stauss HJ. CD8alpha/alpha homodimers fail to function as co-receptor for a CD8-dependent TCR. Eur J Immunol 2007;37:1634–1641. [PubMed: 17506031]
17. Cheroutre H, Lambolez F. Doubting the TCR coreceptor function of CD8alphaalpha. Immunity 2008;28:149–159. [PubMed: 18275828]
18. Crooks ME, Littman DR. Disruption of T lymphocyte positive and negative selection in mice lacking the CD8 beta chain. Immunity 1994;1:277–285. [PubMed: 7889415]
19. Fung-Leung WP, Schilham MW, Rahemtulla A, Kundig TM, Vollenweider M, Potter J, van Ewijk W, Mak TW. CD8 is needed for development of cytotoxic T cells but not helper T cells. Cell 1991;65:443–449. [PubMed: 1673361]
20. Nakayama K, Negishi I, Kuida K, Louie MC, Kanagawa O, Nakauchi H, Loh DY. Requirement for CD8 beta chain in positive selection of CD8-lineage T cells. Science 1994;263:1131–1133. [PubMed: 8108731]
21. Terry LA, DiSanto JP, Small TN, Flomenberg N. Differential expression and regulation of the human CD8 alpha and CD8 beta chains. Tissue Antigens 1990;35:82–91. [PubMed: 2111591]
22. Moebius U, Kober G, Griscelli AL, Hercend T, Meuer SC. Expression of different CD8 isoforms on distinct human lymphocyte subpopulations. Eur J Immunol 1991;21:1793–1800. [PubMed: 1831127]
23. Van Laethem F, Sarafova SD, Park JH, Tai X, Pobezinsky L, Guinter TI, Adoro S, Adams A, Sharrow SO, Feigenbaum L, Singer A. Deletion of CD4 and CD8 coreceptors permits generation of alphabetaT cells that recognize antigens independently of the MHC. Immunity 2007;27:735–750. [PubMed: 18023370]
24. Gao GF, Jakobsen BK. Molecular interactions of coreceptor CD8 and MHC class I: the molecular basis for functional coordination with the T-cell receptor. Immunol Today 2000;21:630–636. [PubMed: 11114424]
25. Gao GF, Willcox BE, Wyer JR, Boulter JM, O'Callaghan CA, Maenaka K, Stuart DI, Jones EY, Van Der Merwe PA, Bell JI, Jakobsen BK. Classical and nonclassical class I major histocompatibility complex molecules exhibit subtle conformational differences that affect binding to CD8alphaalpha. J Biol Chem 2000;275:15232–15238. [PubMed: 10809759]
26. Kern P, Hussey RE, Spoerl R, Reinherz EL, Chang HC. Expression, purification, and functional analysis of murine ectodomain fragments of CD8alphaalpha and CD8alphabeta dimers. J Biol Chem 1999;274:27237–27243. [PubMed: 10480942]
27. Huang J, Edwards LJ, Evavold BD, Zhu C. Kinetics of MHC-CD8 interaction at the T cell membrane. J Immunol 2007;179:7653–7662. [PubMed: 18025211]
28. Bosselut R, Feigenbaum L, Sharrow SO, Singer A. Strength of signaling by CD4 and CD8 coreceptor tails determines the number but not the lineage direction of positively selected thymocytes. Immunity 2001;14:483–494. [PubMed: 11336693]
29. Witte T, Spoerl R, Chang HC. The CD8beta ectodomain contributes to the augmented coreceptor function of CD8alphabeta heterodimers relative to CD8alphaalpha homodimers. Cell Immunol 1999;191:90–96. [PubMed: 9973530]

30. Merry AH, Gilbert RJ, Shore DA, Royle L, Miroshnychenko O, Vuong M, Wormald MR, Harvey DJ, Dwek RA, Classon BJ, Rudd PM, Davis SJ. O-glycan sialylation and the structure of the stalk-like region of the T cell co-receptor CD8. J Biol Chem 2003;278:27119–27128. [PubMed: 12676960]

31. Moody AM, Chui D, Reche PA, Priatel JJ, Marth JD, Reinherz EL. Developmentally regulated glycosylation of the CD8alphabeta coreceptor stalk modulates ligand binding. Cell 2001;107:501–512. [PubMed: 11719190]

32. Wong JS, Wang X, Witte T, Nie L, Carvou N, Kern P, Chang HC. Stalk region of beta-chain enhances the coreceptor function of CD8. J Immunol 2003;171:867–874. [PubMed: 12847256]

33. Rettig L, McNeill L, Sarner N, Guillaume P, Luescher I, Tolaini M, Kioussis D, Zamoyska R. An essential role for the stalk region of CD8beta in the coreceptor function of CD8. J Immunol 2009;182:121–129. [PubMed: 19109142]

34. Mallaun M, Naeher D, Daniels MA, Yachi PP, Hausmann B, Luescher IF, Gascoigne NR, Palmer E. The T cell receptor's alpha-chain connecting peptide motif promotes close approximation of the CD8 coreceptor allowing efficient signal initiation. J Immunol 2008;180:8211–8221. [PubMed: 18523287]

35. Salter RD, Norment AM, Chen BP, Clayberger C, Krensky AM, Littman DR, Parham P. Polymorphism in the alpha 3 domain of HLA-A molecules affects binding to CD8. Nature 1989;338:345–347. [PubMed: 2784196]

36. Potter TA, Rajan TV, Dick RF 2nd, Bluestone JA. Substitution at residue 227 of H-2 class I molecules abrogates recognition by CD8-dependent, but not CD8-independent, cytotoxic T lymphocytes. Nature 1989;337:73–75. [PubMed: 2462676]

37. Potter TA, Bluestone JA, Rajan TV. A single amino acid substitution in the alpha 3 domain of an H-2 class I molecule abrogates reactivity with CTL. J Exp Med 1987;166:956–966. [PubMed: 3498790]

38. Salter RD, Benjamin RJ, Wesley PK, Buxton SE, Garrett TP, Clayberger C, Krensky AM, Norment AM, Littman DR, Parham P. A binding site for the T-cell co-receptor CD8 on the alpha 3 domain of HLA-A2. Nature 1990;345:41–46. [PubMed: 2109837]

39. Connolly JM, Hansen TH, Ingold AL, Potter TA. Recognition by CD8 on cytotoxic T lymphocytes is ablated by several substitutions in the class I alpha 3 domain: CD8 and the T-cell receptor recognize the same class I molecule. Proc Natl Acad Sci U S A 1990;87:2137–2141. [PubMed: 2107545]

40. Connolly JM, Potter TA, Wormstall EM, Hansen TH. The Lyt-2 molecule recognizes residues in the class I alpha 3 domain in allogeneic cytotoxic T cell responses. J Exp Med 1988;168:325–341. [PubMed: 2456371]

41. Sanders SK, Fox RO, Kavathas P. Mutations in CD8 that affect interactions with HLA class I and monoclonal anti-CD8 antibodies. J Exp Med 1991;174:371–379. [PubMed: 1906921]

42. Gao GF, Tormo J, Gerth UC, Wyer JR, McMichael AJ, Stuart DI, Bell JI, Jones EY, Jakobsen BK. Crystal structure of the complex between human CD8alpha(alpha) and HLA-A2. Nature 1997;387:630–634. [PubMed: 9177355]

43. Devine L, Sun J, Barr MR, Kavathas PB. Orientation of the Ig domains of CD8 alpha beta relative to MHC class I. J Immunol 1999;162:846–851. [PubMed: 9916707]

44. Chang HC, Tan K, Hsu YM. CD8alphabeta has two distinct binding modes of interaction with peptide-major histocompatibility complex class I. J Biol Chem 2006;281:28090–28096. [PubMed: 16840780]

45. Devine L, Thakral D, Nag S, Dobbins J, Hodsdon ME, Kavathas PB. Mapping the binding site on CD8 beta for MHC class I reveals mutants with enhanced binding. J Immunol 2006;177:3930–3938. [PubMed: 16951356]

46. Li H, Natarajan K, Malchiodi EL, Margulies DH, Mariuzza RA. Three-dimensional structure of H-2D^{d} complexed with an immunodominant peptide from human immunodeficiency virus envelope glycoprotein 120. J Mol Biol 1998;283:179–191. [PubMed: 9761682]

47. Hogquist KA, Tomlinson AJ, Kieper WC, McGargill MA, Hart MC, Naylor S, Jameson SC. Identification of a naturally occurring ligand for thymic positive selection. Immunity 1997;6:389–399. [PubMed: 9133418]

48. Kern PS, Teng MK, Smolyar A, Liu JH, Liu J, Hussey RE, Spoerl R, Chang HC, Reinherz EL, Wang JH. Structural basis of CD8 coreceptor function revealed by crystallographic analysis of a murine

CD8alphaalpha ectodomain fragment in complex with H-2Kb. Immunity 1998;9:519–530. [PubMed: 9806638]

49. Chang HC, Tan K, Ouyang J, Parisini E, Liu JH, Le Y, Wang X, Reinherz EL, Wang JH. Structural and mutational analyses of a CD8alphabeta heterodimer and comparison with the CD8alphaalpha homodimer. Immunity 2005;23:661–671. [PubMed: 16356863]
50. Corr M, Slanetz AE, Boyd LF, Jelonek MT, Khilko S, al-Ramadi BK, Kim YS, Maher SE, Bothwell AL, Margulies DH. T cell receptor-MHC class I peptide interactions: affinity, kinetics, and specificity. Science 1994;265:946–949. [PubMed: 8052850]
51. Otwinowski, Z.; Minor, W. Processing of X-ray diffraction data collected in oscillation mode. In: Carter, JCW.; Sweet, RM., editors. Methods in Enzymology. Academic Press; New York: 1997. p. 307-326.
52. Vagin A, Teplyakov A. MOLREP: an automated program for molecular replacement. J Appl Cryst 1997;30:1022–1025.
53. McCoy AJ, Grosse-Kunstleve RW, Adams PD, Winn MD, Storoni LC, Read RJ. Phaser crystallographic software. J Appl Cryst 2007;40:658–674. [PubMed: 19461840]
54. CCP4. Collaborative Computation Project; The CCP4 Suite: Programs for Protein Crystallography. Acta Cryst 1994;D50:760–763.
55. Tormo J, Natarajan K, Margulies DH, Mariuzza RA. Crystal structure of a lectin-like natural killer cell receptor bound to its MHC class I ligand. Nature 1999;402:623–631. [PubMed: 10604468]
56. Berman HM, Westbrook J, Feng Z, Gilliland G, Bhat TN, Weissig H, Shindyalov IN, Bourne PE. The Protein Data Bank. Nucleic Acids Res 2000;28:235–242. [PubMed: 10592235]
57. Emsley P, Cowtan K. Coot: model-building tools for molecular graphics. Acta Crystallogr D Biol Crystallogr 2004;60:2126–2132. [PubMed: 15572765]
58. Brunger AT. Version 1.2 of the Crystallography and NMR system. Nat Protoc 2007;2:2728–2733. [PubMed: 18007608]
59. Adams PD, Grosse-Kunstleve RW, Hung LW, Ioerger TR, McCoy AJ, Moriarty NW, Read RJ, Sacchettini JC, Sauter NK, Terwilliger TC. PHENIX: building new software for automated crystallographic structure determination. Acta Crystallogr D Biol Crystallogr 2002;58:1948–1954. [PubMed: 12393927]
60. Laskowski RA, Hutchinson EG, Michie AD, Wallace AC, Jones ML, Thornton JM. PDBsum: a Web-based database of summaries and analyses of all PDB structures. Trends Biochem Sci 1997;22:488–490. [PubMed: 9433130]
61. Moody AM, Xiong Y, Chang HC, Reinherz EL. The CD8alphabeta co-receptor on double-positive thymocytes binds with differing affinities to the products of distinct class I MHC loci. Eur J Immunol 2001;31:2791–2799. [PubMed: 11536178]
62. Wooldridge L, van den Berg HA, Glick M, Gostick E, Laugel B, Hutchinson SL, Milicic A, Brenchley JM, Douek DC, Price DA, Sewell AK. Interaction between the CD8 coreceptor and major histocompatibility complex class I stabilizes T cell receptor-antigen complexes at the cell surface. J Biol Chem 2005;280:27491–27501. [PubMed: 15837791]
63. Cai Z, Brunmark AB, Luxembourg AT, Garcia KC, Degano M, Teyton L, Wilson I, Peterson PA, Sprent J, Jackson MR. Probing the activation requirements for naive CD8+ T cells with Drosophila cell transfectants as antigen presenting cells. Immunol Rev 1998;165:249–265. [PubMed: 9850865]
64. Yachi PP, Ampudia J, Zal T, Gascoigne NR. Altered peptide ligands induce delayed CD8-T cell receptor interaction--a role for CD8 in distinguishing antigen quality. Immunity 2006;25:203–211. [PubMed: 16872849]
65. Liu Y, Xiong Y, Naidenko OV, Liu JH, Zhang R, Joachimiak A, Kronenberg M, Cheroutre H, Reinherz EL, Wang JH. The crystal structure of a TL/CD8alphaalpha complex at 2.1 A resolution: implications for modulation of T cell activation and memory. Immunity 2003;18:205–215. [PubMed: 12594948]
66. Lawrence MC, Colman PM. Shape complementarity at protein/protein interfaces. J Mol Biol 1993;234:946–950. [PubMed: 8263940]
67. Achour A, Persson K, Harris RA, Sundback J, Sentman CL, Lindqvist Y, Schneider G, Karre K. The crystal structure of H-2Dd MHC class I complexed with the HIV-1-derived peptide P18-I10 at 2.4

A resolution: implications for T cell and NK cell recognition. Immunity 1998;9:199–208. [PubMed: 9729040]

68. Devine L, Rogozinski L, Naidenko OV, Cheroutre H, Kavathas PB. The complementarity-determining region-like loops of CD8 alpha interact differently with beta 2-microglobulin of the class I molecules H-2Kb and thymic leukemia antigen, while similarly with their alpha 3 domains. J Immunol 2002;168:3881–3886. [PubMed: 11937542]
69. Sekimata M, Tanabe M, Sarai A, Yamamoto J, Kariyone A, Nakauchi H, Egawa K, Takiguchi M. Different effects of substitutions at residues 224 and 228 of MHC class I on the recognition of CD8. J Immunol 1993;150:4416–4426. [PubMed: 8482843]
70. Durairaj M, Sharma R, Varghese JC, Kane KP. Requirement for Q226, but not multiple charged residues, in the class I MHC CD loop/D strand for TCR-activated CD8 accessory function. Eur J Immunol 2003;33:676–684. [PubMed: 12616488]
71. Cohen CJ, Li YF, El-Gamil M, Robbins PF, Rosenberg SA, Morgan RA. Enhanced antitumor activity of T cells engineered to express T-cell receptors with a second disulfide bond. Cancer Res 2007;67:3898–3903. [PubMed: 17440104]
72. Cohen CJ, Zhao Y, Zheng Z, Rosenberg SA, Morgan RA. Enhanced antitumor activity of murine-human hybrid T-cell receptor (TCR) in human lymphocytes is associated with improved pairing and TCR/CD3 stability. Cancer Res 2006;66:8878–8886. [PubMed: 16951205]
73. Blue ML, Craig KA, Anderson P, Branton KR Jr, Schlossman SF. Evidence for specific association between class I major histocompatibility antigens and the CD8 molecules of human suppressor/cytotoxic cells. Cell 1988;54:413–421. [PubMed: 2969292]
74. Santos SG, Powis SJ, Arosa FA. Misfolding of major histocompatibility complex class I molecules in activated T cells allows cis-interactions with receptors and signaling molecules and is associated with tyrosine phosphorylation. J Biol Chem 2004;279:53062–53070. [PubMed: 15471856]
75. Gaspar R Jr, Bagossi P, Bene L, Matko J, Szollosi J, Tozser J, Fesus L, Waldmann TA, Damjanovich S. Clustering of class I HLA oligomers with CD8 and TCR: three-dimensional models based on fluorescence resonance energy transfer and crystallographic data. J Immunol 2001;166:5078–5086. [PubMed: 11290789]
76. Bushkin Y, Demaria S, Le JM, Schwab R. Physical association between the CD8 and HLA class I molecules on the surface of activated human T lymphocytes. Proc Natl Acad Sci U S A 1988;85:3985–3989. [PubMed: 3131769]
77. Mancebo E, Moreno-Pelayo MA, Mencia A, de la Calle-Martin O, Allende LM, Sivadorai P, Kalaydjieva L, Bertranpetit J, Coto E, Calleja-Antolin S, Ruiz-Contreras J, Paz-Artal E. Gly111Ser mutation in CD8A gene causing CD8 immunodeficiency is found in Spanish Gypsies. Mol Immunol 2008;45:479–484. [PubMed: 17658607]
78. de la Calle-Martin O, Hernandez M, Ordi J, Casamitjana N, Arostegui JI, Caragol I, Ferrando M, Labrador M, Rodriguez-Sanchez JL, Espanol T. Familial CD8 deficiency due to a mutation in the CD8 alpha gene. J Clin Invest 2001;108:117–123. [PubMed: 11435463]
79. Lee B, Richards FM. The interpretation of protein structures: estimation of static accessibility. J Mol Biol 1971;55:379–400. [PubMed: 5551392]
80. Saff EB, Kuijlaars ABJ. Distributing many points on a sphere. The Mathematical Intelligencer 1997;19:5–11.
81. Attinger A, Devine L, Wang-Zhu Y, Martin D, Wang JH, Reinherz EL, Kronenberg M, Cheroutre H, Kavathas P. Molecular basis for the high affinity interaction between the thymic leukemia antigen and the CD8alphaalpha molecule. J Immunol 2005;174:3501–3507. [PubMed: 15749886]
82. Laskowski RA. PDBsum new things. Nucleic Acids Res 2009;37:D355–359. [PubMed: 18996896]
83. Gouet P, Robert X, Courcelle E. ESPript/ENDscript: Extracting and rendering sequence and 3D information from atomic structures of proteins. Nucleic Acids Res 2003;31:3320–3323. [PubMed: 12824317]

Abbreviations used in this paper

β2m β2-microglobulin

MHCI	MHC class I molecule
MHCII	MHC class II molecule
$p56^{lck}$	Lc kinase
CDR	complementarity determining region

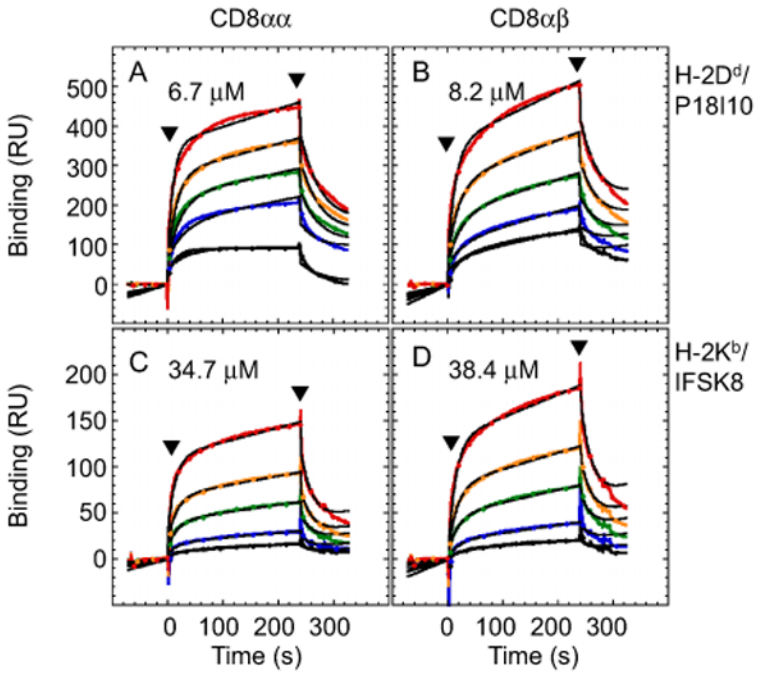

Figure 1.

Binding of MHC/peptide complexes to CD8αα and CD8αβ.

CD8αα and CD8αβ were coupled to the dextran surface of a CM5 biosensor chip by standard amine coupling chemistry, and increasing concentrations (1μM, 2μM, 5μM, 10μM, 20μM) of either H-2D^d or H-2K^b were sequentially injected over each surface. The zero time point corresponds to the start of the injection of the soluble analyte. Buffer washout was initiated at 240 seconds. Background binding to a mock-coupled surface was subtracted. The peptides bound to H-2D^d and H-2K^b are P18-I10 (RGPGRAFVTI) and IFSK8 (ISFKFDHL) respectively. Calculated K_D values based on a simple monovalent interaction model, AB <---->A + B, were determined from both kinetics and steady-state evaluation of global curve fits using BIAeval 3.2. Data points collected at 5 Hz are plotted in color and corresponding curve fits are in black.

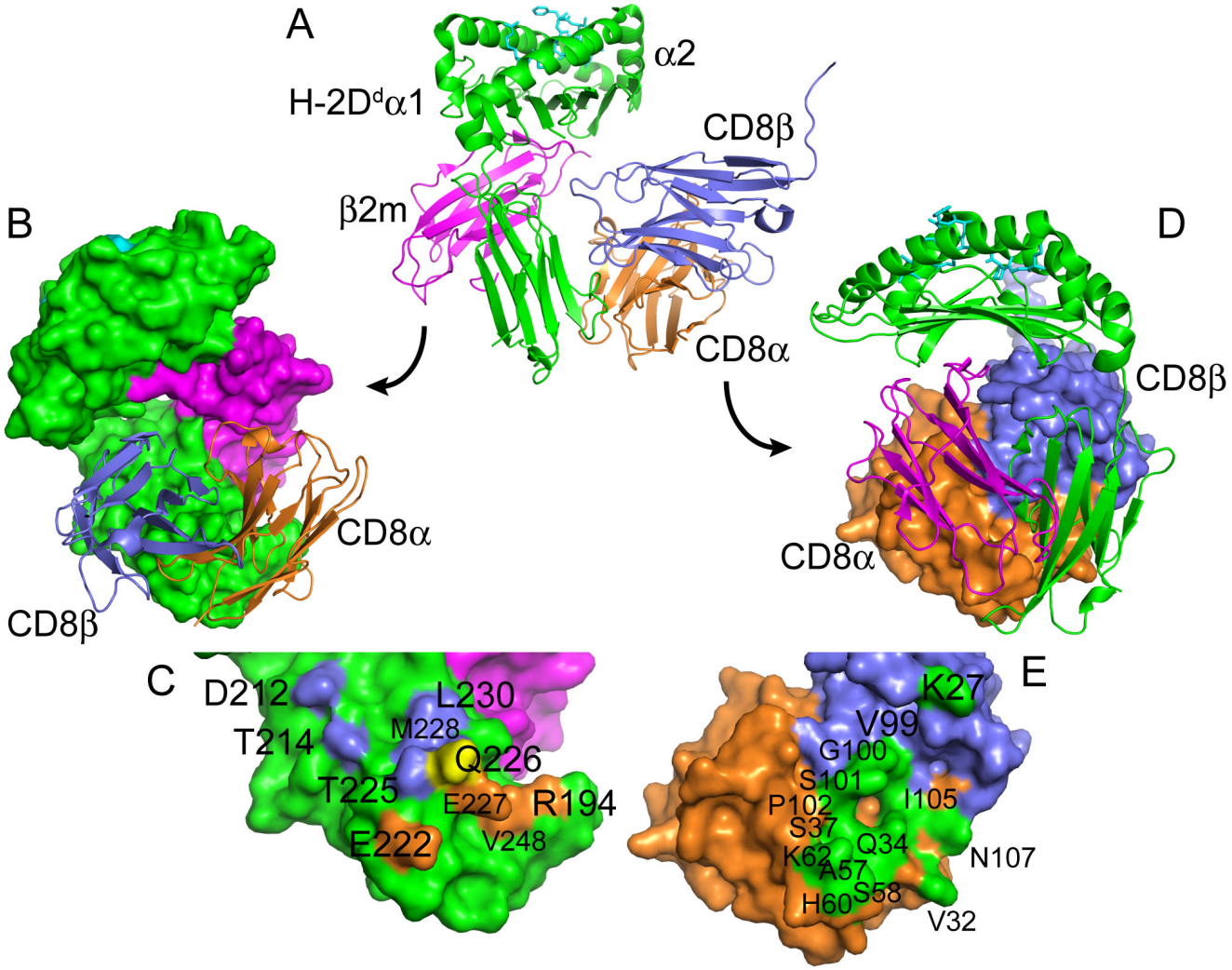

Figure 2.

Structure of CD8αβ /H-2D^d/P18I10 complex.

Graphics representation of the CD8αβ/H-2D^d/P18I10 complex is shown in ribbon representation (A) colored as H-2D^d heavy chain (green), β2m light chain (magenta), bound P18I10 peptide (light blue), CD8α (orange), and CD8β (slate). Panel (B) shows a rotation about the y axis of about 90°, with the MHC complex in a surface representation, and the CD8αβ heterodimer as ribbons. Panel (C) shows a close-up of the H-2D^d residues that contact CD8. Residues that contact the CD8α chain are shown in orange, and those that contact CD8β are in slate. The single residue, Q226, that contacts both CD8 chains is yellow. Panel (D) is a rotation of (A) of about -90°, with the CD8 heterodimer in a surface representation, and the MHC in ribbons. Panel (E) reveals the residues of CD8 that contact the MHC, colored in green.

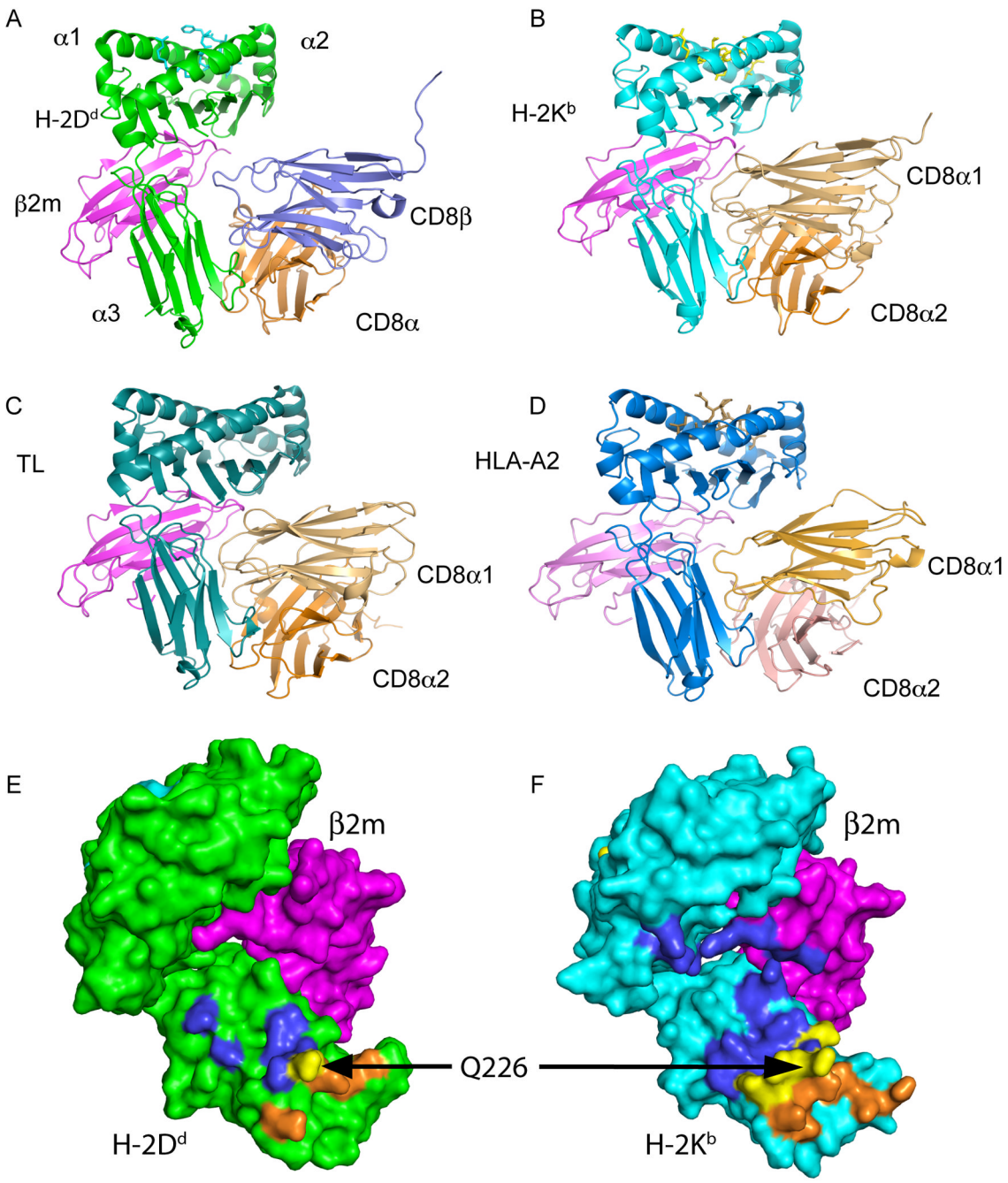

Figure 3.

Comparison of CD8αβ/H-2D^d complex to other CD8/MHC complexes. Structures of CD8αα/H-2K^b (1BQH) (48), CD8αα/TL (1NEZ) (81), and CD8αα/HLA-A2 (1AKJ) (42) were each superposed on CD8αβ/H-2D^d, and are illustrated here as ribbon diagrams in the same orientation. (A) shows ribbon diagram of CD8αβ/H-2D^d; (B) CD8αα/H-2K^b; (C) CD8αα/TL; (D) CD8αα/HLA-A2. Panel E illustrates the footprint of CD8αβ on H-2D^d/β2m, with the residues contacting CD8β colored blue, those contacting CD8α colored orange, and the single residue (Q226) contacted by both in yellow. Panel F shows the footprint of CD8αα on H-2K^b/β2m, with the residues contacting CD8α1 in blue, those contacting CD8α2 in orange and those contacting both CD8α subunits in yellow.

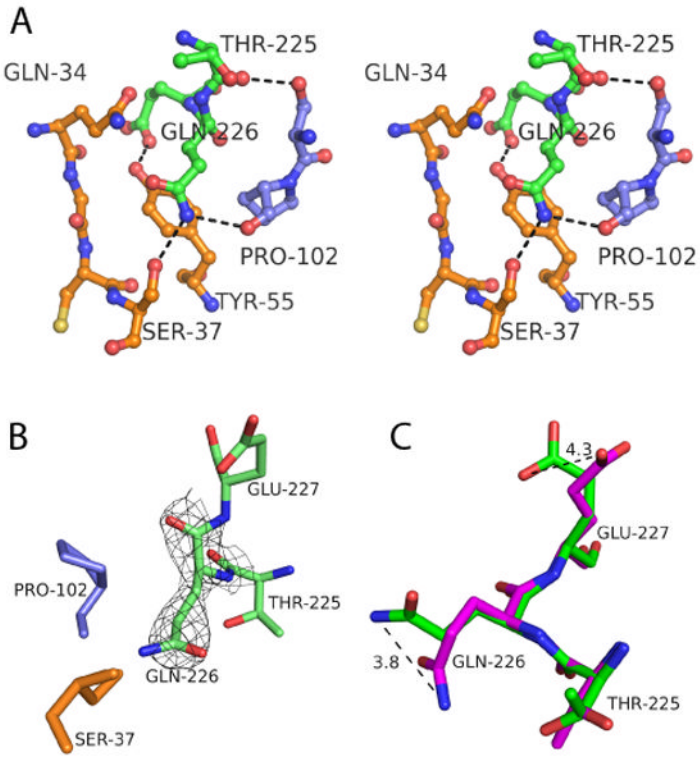

Figure 4.

Close-up examination of residues of the CD8αβ/H-2D^d interface.

Panel (A) is a side-by-side stereo view of the intimate interaction of Gln226 of the MHC heavy chain with residues of both chains of CD8. Panel (B) shows Gln226 of H-2D^d and the corresponding density map contoured at 1.5 σ, illustrating the proximity to CD8α Ser37 and CD8β Pro102. Panel (D) shows residues 225 to 227 of H-2D^d of the CD8αβ/H-2D^d complex (green) superposed on the same residues of the unliganded 1.7 Å H-2D^d structure (purple). Movements of the Nε of Gln226 of 3.8 Å and of the Oε1 (4.3 Å) of Glu227 are indicated.

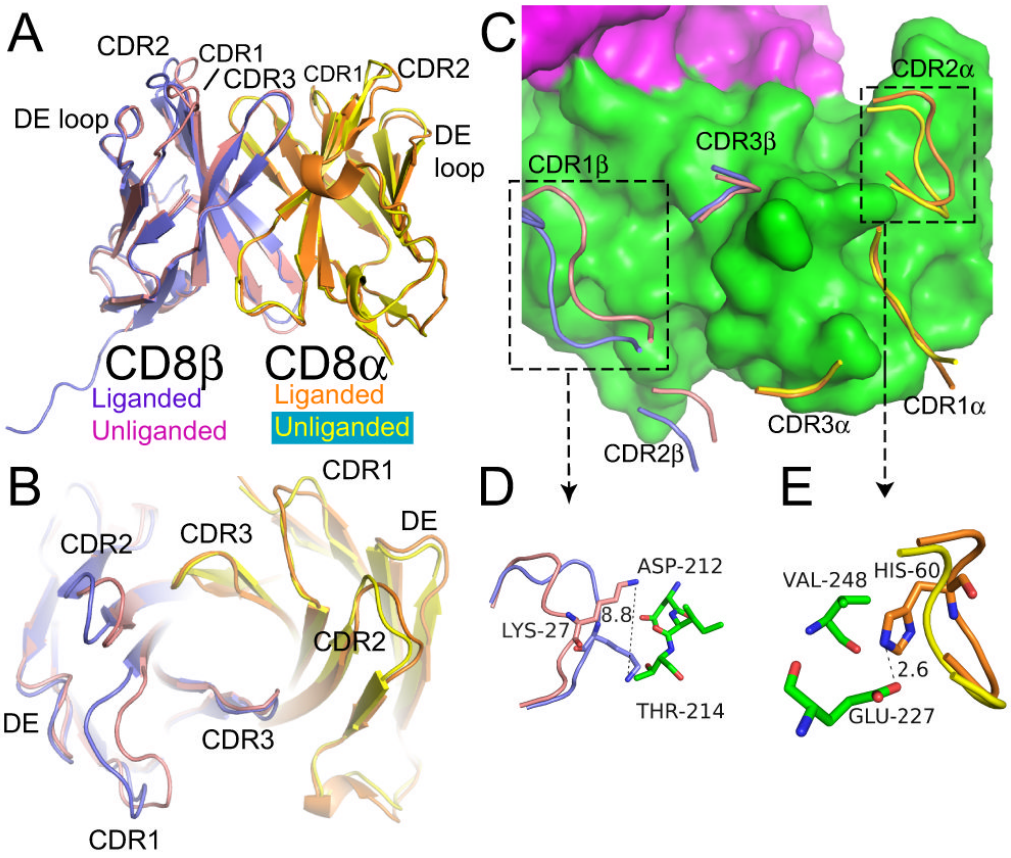

Figure 5.

Comparison of bound and free CD8αβ.

(A) Coordinates of mouse CD8αβ free (2ATP(49)) were superposed onto the CD8αβ heterodimer in the complex. CD8α and CD8β in the bound complex are orange and slate respectively, and in the unbound state are yellow and pink. Loop designations are shown in a structure based sequence alignment in Fig. S2. (B) The CDR loops, as indicated, are shown in tube representation, and (C) shows CDR loops in the context of the H-2D^d structure. (D) shows an edited close-up of the interactions between CD8β CDR1 Lys27 liganded (slate) and H-2D^d (green). (E) shows the movement of the CD8α CDR2 loop, focused on residue H60.

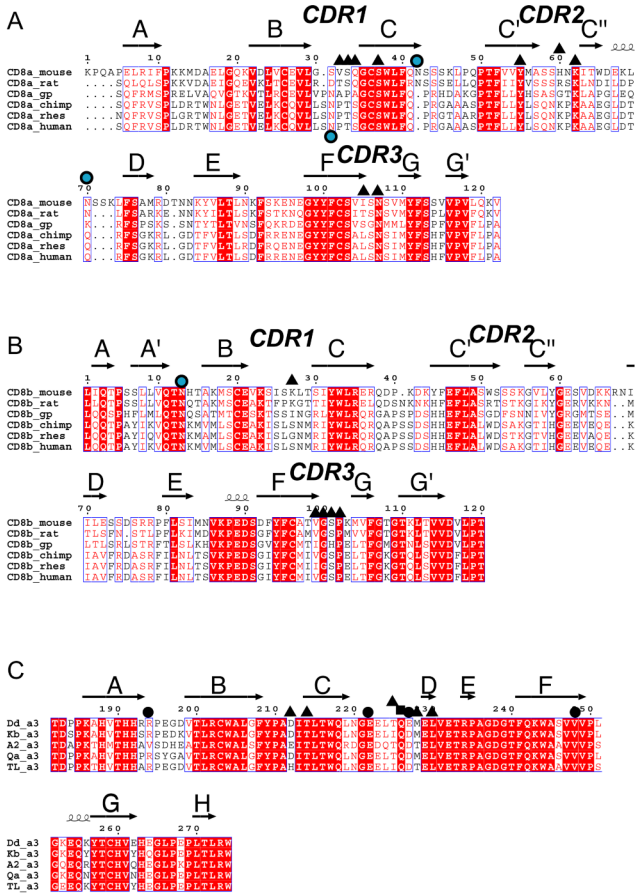

Figure 6.

Structure-based sequence alignment of CD8α, CD8β, and the α3 domain of MHCI. The indicated sequences were aligned as described (83). (A) CD8α alignment. CD8α residues that contact or form hydrogen bonds to MHCI heavy chain are shown as black triangles. Green filled circles are potential N-asparaginyl-glycosylation sites. (B) CD8β alignment. CD8β residues that contact H-2D^d in the CD8αβ/H-2D^d complex are shown as black filled triangles. Green filled circles are potential glycosylation sites. (C) MHCI α3 domain alignment. Indicated residues are: filled circles, H-2D^d α3 domain residues of CD8αβ/H-2D^d that contact CD8α; filled triangles, H-2D^d α3 domain residues of CD8αβ/H-2D^d that contact CD8β; and filled square, H-2D^d α3 domain residue of CD8αβ/H-2D^d that contacts both CD8α and CD8β.

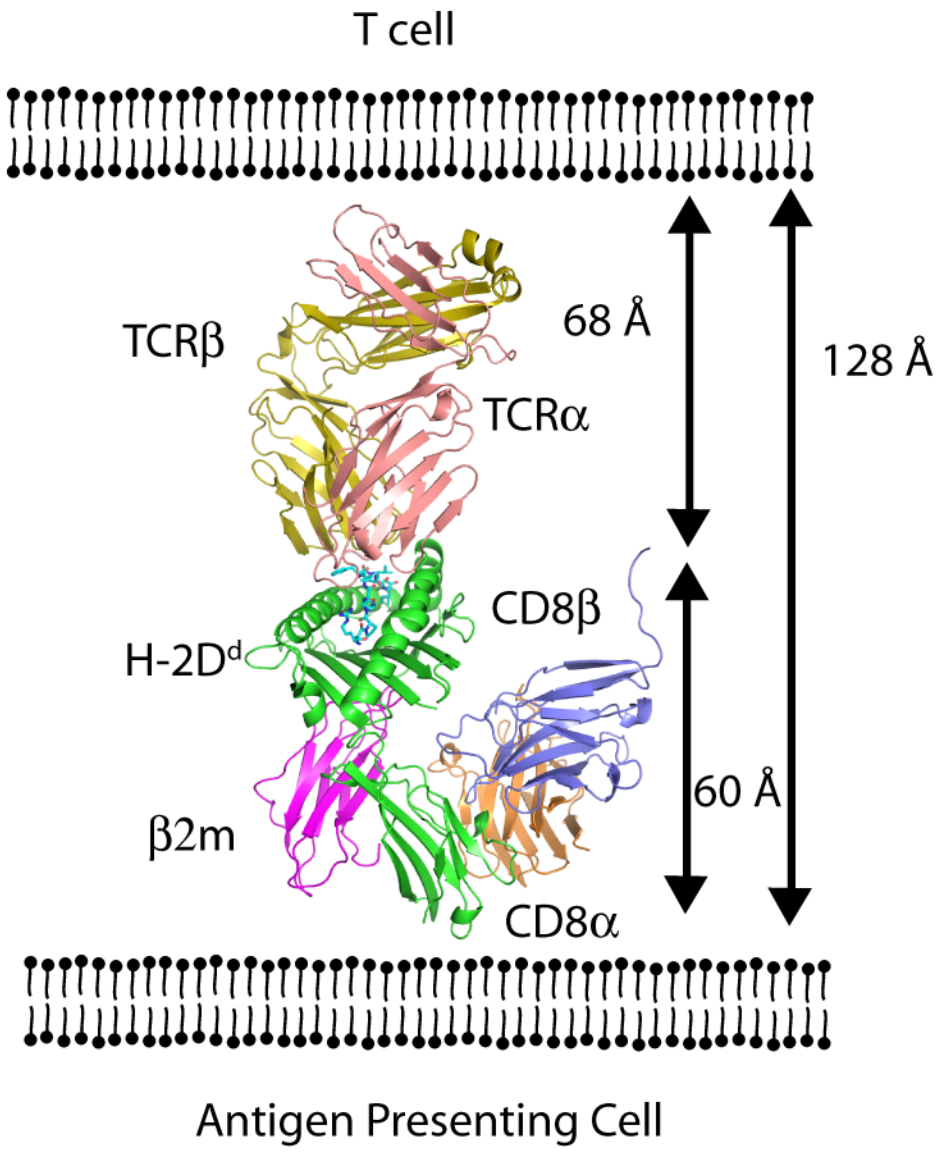

Figure 7.

Schematic illustration of distance of CD8αβ from apposed T cell, based on superposition of TCR/MHC complex onto CD8αβ/MHCI complex. Coordinates of the H-2D^d moiety of a P18I10-specific TCR in complex with H-2D^d/β2m/P18I10 determined to 2.0 Å resolution (K.N. and D.H.M., unpublished data) were superposed on the H-2D^d of the CD8αβ/H-2D^d complex using PyMOL (http://www.pymol.org). Stalk regions of CD8α and β as well as transmembrane regions of the indicated chains are shown as dashed lines.

Table I

Data collection and refinement statistics [a]

	CD8αβ /H-2D[d]	H-2D[d]
Data collection		
Space group	P $2_12_12_1$	P $2_12_12_1$
Cell dimensions		
a, b, c (Å)	79.47, 96.69, 97.54	46.72, 89.45, 109.70
α, β, γ (°)	90.0, 90.0, 90.0	90.0, 90.0, 90.0
Resolution (Å)	100-2.6 (2.6) [*]	30-1.7
R_{sym} or R_{merge}	5.7 (43.2)	6.4 (44.1)
I / σI	17.4 (2.6)	21.5 (3.7)
Completeness (%)	96.1 (76.9)	95.0 (68.9)
Redundancy	6.4 (4.2)	11.1 (5.9)
Refinement		
Resolution (Å)	2.6	1.7
No. reflections	23,833	48,991
R_{work} / R_{free}	24.8/29.2	18.3/22.7
No. atoms		
Protein	5059	3155
Ligand/ion		1
Water	37	316
B-factors (Å^2)		
Protein	54.7	33.4
Ligand/ion		
Water	43.4	42.4
R.m.s. deviations		
Bond lengths (Å)	0.01	0.005
Bond angles (°)	2.1	1.0

[a] Each data set was collected on a single crystal.

[*] Values in parentheses are for highest-resolution shell.

Table II

[a] Interactions between CD8αβ and H-2D[d]

Hydrogen bonds		
CD8αβ	H-2D[d]	Length (Å)
CD8α		
Ser37 Oγ Tyr55 Oη	Gln226 Nε2 Glu227 Oε1	2.9 2.4
CD8β		
Ser101 Oγ Pro102 O	Thr225 O Gln226 Nε2	2.7 3.0
Contacts between CD8αβ and H-2D[d] (distances < 4.0 Å)		
Structural element	CD8αβ	H-2D[d]
CD8α		
CDR1	Val32 (1) Gln34 (11)	E222 Q226, E227
β-strand C′	Tyr55 (8)	Q226, E227
CDR2	A57 (4) S58 (1) H60 (11) K62 (3)	E227 E227 E227, V248, R194 V248
CDR3	I105 (1) N107 (9) (total non-bonded =48)	E222 E222
CD8β		
CDR1	K27 (5)	D212, T214 (BC loop)
β-strand F	V99 (1)	T225, Q226
CDR3	G100 (3) S101 (8) P102 (6) (total non-bonded = 23)	T225, Q226 T225, M228, L230 Q226

[a] Contacting atoms were calculated as described in Materials and Methods. Number of non-bonded contacts is given in parenthesis following the residue designation.

Table III

Buried Surface Areas of CD8αβ/H-2D^{d} Subunit Interfaces[a]

	H-2K^{b}	TL	HLA-A2	H-2D^{d}
CD8αα	1756 CD8α1:1205 (69%) CD8α2: 689	1855 CD8α1: 1327 (71%) CD8α2: 676	1302 CD8α1: 963 (74%) CD8α2: 454	N/A
CD8αβ	N/A	N/A	N/A	963 CD8β: 473 (49%) CD8α: 590

[a]Buried surface areas in Å^{2} were calculated with AREAIMOL of the CCP4 suite (54,79,80), using a 1.7Å probe radius. Structures used were protein data bank (PDB (56)) designations: 1BQH (48), 1NEZ (81), and 1AKJ (42) for complexes with H-2K^{b}, TL, and and HLA-A2 respectively. N/A, not available. Values in parenthesis indicate the percentage of the total interface area contributed by the individual subunits.

Table IV

Structural interpretation of effects of mutations of CD8 and MHC on CD8 binding and function.

	Experimental System	Molecule Tested[a]	Mutation	Effect[b]	Structural Interpretation[c]	Reference
Protein						
CD8α	Tetramer of TL or K^b (with hβ2m) on CD8αα of COS-7 transfectants	CD8αα mutants	TL binding			(68)
			N107A	↓	Contact CD8α1 to TL T228, E229, L230; CD8α2 to TL E222	
			K62E	↓↓	Contact CD8α2 to R194, V248	
			S31L, S31A	↓↓, ↓	Contact CD8α1 to L 230, E232, T233, K243	
			K^b binding			
			K73A	↑↑	Not at CD8/K^b interface; no simple explanation	
			N107A	↓↓	Contact CD8α1 to M228, E229, L230; CD8α2 to E222	
			T81A	↓	no simple explanation; at border of CD8α1/K^b interface	
			K62E	↓↓	Contact CD8α2 to K^b E229	
			S31L, S31A	↓↓, ↓↓	Contact CD8α1 to K^b E232, T233, K243	
			L29A	↓	No contacts, no simple explanation	
			K12E	↓	No contacts, no simple explanation	
			R8D, R8A	↓↓, ↓↓	CD8α1 contact to β2m K58, β2m D59	
	T cell hybridoma stimulation	CD8αα mutants	R8A	↓↓	CD8α1 contact to β2m K58, β2m D59	(32)
	T cell hybridoma stimulation	CD8αα mutants	E27A	↓↓	CD8α1 contact to β2m K58	(44)
CD8β	Tetramer of K^b (with hβ2m) on CD8αβ of COS-7 transfectants	CD8αβ (β mutants)	β mutant		(Explanations based on CD8αβ/H-2D^d structure)	(45)
			K103D	↓	No contact; possible salt bridge with CD8α D66; ? dimer stability	
			S101A	↓	Contacts to T225, M228, L230	
			V99R	↓	Contacts to T225; ? dimer stabilization via CD8α M110	
			L58R	↑	No contact to D^d; Contact to CD8α S108	
			K55D	↓	No contact to D^d; Contact to CD8α S108	
			S53L	↑	No contact; ? stabilization of CD8β CDR2 loop	
			K23D	↓	No contact; no effect of K23A	
	T cell hybridoma stimulation	CD8β mutants with $CD8\alpha^{R8A}$	β mutant			(49)
			I25A	No effect	No contacts to D^d	
			T29A	No effect	No contacts to D^d	
			L28A	No effect	No contacts to D^d	
			V57A	No effect	No contacts to D^d	
			S53A	↓	No contacts to D^d	
			S54A	↓	No contacts to D^d	
			K55A	↓↓↓	No contacts to D^d; Contact to CD8α S108; ? dimerization	
			G56A	↓	No contacts to D^d	
			K103A	↓↓	No contacts to D^d; Contact to CD8α D66; ? dimerization	
			P102A	↓↓↓	Contacts to D^d Q226; Contact to CD8α F52, Y55, T64	
			S101A	↓↓↓	Contacts to D^d T225, M228, L230	
	T cell hybridoma	CD8 β mutants with wt α	β mutant with wt α			(44)
			K55A	↓	No contacts to D^d; Contact to CD8α S108; ? dimerization	

	Experimental System	Molecule Tested[a]	Mutation	Effect[b]	Structural Interpretation[c]	Reference
Protein						
			K103A	↓	No contacts to D^d; Contact to CD8α D66; ? dimerization	
			S101A	↓↓	Contacts to D^d T225, M228, L230	
MHC mutants	Alloreactive anti-D^d CTL	D^d mutant with CD8αβ CTL	D^d mutant			(36,37,39)
			E227K	↓↓	Contact to CD8α Q34, Y55, A57, S58, H60; charge reversal	
			H192D	no effect	No contact	
			E222K	↓	Contact to CD8α V32, I105, N107; charge reversal	
			E223K	↓	No contact, but charge reversal near contact	
			E227D	no effect	Conservative substitution, interaction preserved	
			E229K	↓	No contact, but charge reversal near contact	
			E232K	no effect	No contact	
			E227R	↓	Contact to CD8α Q34, Y55, A57, S58, H60; charge reversal	
			E227H	↓	Contact to CD8α Q34, Y55, A57, S58, H60	
			E227Y	↓	"	
			E227A	↓	"	
			E227L	↓	"	
			E227P	↓	"	
			E227F	↓	"	
MHC mutants	CTL (antigen-specific)	D^d mutant with CD8αβ CTL	E227K	↓	Contact to CD8α Q34, Y55, A57, S58, H60; charge reversal	(13)
	CTL and hybridoma (allo-anti-K^b)	K^b and K^b/HLA-B7 chimeras	K^b mutant			(69)
			E223D	↑	No contacts; preserves charge	
			L224Q	↓	Contact to CD8α Q34 in CD8αβ/D^d complex	
			M228T	CTL↓; IL-2 no change.	Contact to CD8β S101 in CD8αβ/D^d complex	
	CTL (allo- anti-K^b)—solid phase purified wt and mutant MHC	K^b/D^d chimeras and mutants--CTL	E222A/ E223A/ E227A	Degran↓Adh↓	No effect on CD8 independent clones; solid phase adhesion and degranulation affected for CD8-dependent cells	(70)
			(triple) E227A/ E229A/ E232A	Degran↓Adh↓	Contact of E222 and E227 with CD8α; No contact of E232	
			(triple) Q226/ E227A (double)	Degran↓Adh↓	Q226 interacts with CD8α CDR1 and CD8β CDR3 and β-strand F	
			Q115A/ D122A (double)	no effect	Residues on floor of MHC α2, no interaction with CD8αβ	
			Q226A	Degran↓Adh↓	Contact to CD8α and CD8β	
			E227A	No effect	Lack of effect of E227A difficult to explain in view of multiple contacts to CD8α	

	Experimental System	Molecule Tested[a]	Mutation	Effect[b]	Structural Interpretation[c]	Reference
Protein						
	T cell hybridoma, K^b, peptide specific	K^b mutants, to CD8αα and CD8αβ	K^b mutant			(32)
			K198A	Subtle effect	Contact to CD8α2 S59	
			Q226A	↓ both CD8αα and CD8αβ	Multiple contacts to CD8αα and CD8αβ	
			D227A	No effect	Consistent with E227A mut of D^d(see above)	
	Tetramer binding of TL, K^b, and TL/K^b chimeras to CD8αα transfectants and IEL	TL, K^b, A2 and TL/K^b chimeras and point mutants	Exon shuffles			(81)
			K^b/TLα3	Strong staining	Multiple contributions from AB and CD loops of TL and/or K^b influence binding and function.	
			A2/TLα3	Strong staining		
			TL D198K	↓	Contacts CD8α2 H60	
			TL G197D	↓↓	Contributions from TL G197D may distort AB loop of TL	
			Dl98K			
			(double)			
			TL G197D	↓	T228 contacts CD8α1 N107, triple mutant affects both CD8α1 and CD8α2 contacts	
			D198K			
			T228M			
			(triple)			
			K^b D197G	↑↑ TL and IEL binding	K198D contacts CD8α2 H60, restores TL-like binding, M228 of K^b contacts N107, S108, and Q34 of CD8α1, T228 of TL contacts N107 of CD8α1	
			K198D			
			M228T			
			(triple)			

[a] Since CTL lines and clones predominantly express CD8αβ, assays involving CTL are interpreted as reflecting CD8αβ function.

[b] Assays: CTL, cytotoxic T lymphocyte; degran, degranulation assay; ad, adhesion; tetramer, staining with MHCI tetramer in TCR independent setting. Up and down arrows indicate increased or decreased recognition in the indicated assay.

[c] Structural interpretations based on structures of CD8αα/TL (1NEZ) (65), CD8αα/H-2K^b (1BQH)(48), and the present study for CD8αβ/H-2D^d, all analyzed with PDBsum (82). Interpretations of 1BQH are based on the first complex in the asymmetric unit.